Polymer 50 (2009) 2065–2074

Contents lists available at ScienceDirect

Polymer

journal homepage: www.elsevier.com/locate/polymer

Dynamic swelling of hydrogels based on random terpolymers of *N*-isopropylacrylamide, methacrylic acid and poly(ethylene glycol) macromonomer

Rodrigo París, José Manuel Barrales-Rienda, Isabel Quijada-Garrido*

Departamento de Química-Física de Polímeros, Instituto de Ciencia y Tecnología de Polímeros (ICTP), Consejo Superior de Investigaciones Científicas (CSIC), C/Juan de la Cierva 3, E-28006 Madrid, Spain

ARTICLE INFO

Article history:
Received 4 August 2008
Accepted 18 February 2009
Available online 26 February 2009

Keywords:
Hydrogel
N-Isopropylacrylamide
Methacrylic acid

ABSTRACT

A series of pH-responsive hydrogels based on *N*-isopropylacrylamide (*N*-iPAAm), methacrylic acid (MAA) and poly(ethylene glycol) monomethyl ether monomethacrylate macromonomer (PEGMEMA), P(*N*-iPAAm-*co*-MAA-*co*-PEGMEMA) random terpolymers, were synthesized and their swelling behaviour studied as a function of both monomer composition and previous swelling treatment. The swelling kinetic curves were followed using gravimetric, photographic and magnetic resonance imaging (MRI) techniques, which provide spatial and temporal resolution. The swelling behaviour was non-Fickian at pH 7, being this fact more relevant when the samples were pre-soaked in pH 2 solution. Low pH promotes hydrogen bond arrangements that disrupt at pH 7, where sigmoidal swelling curves were observed. The sigmoidal shape of the curves increases as well as the swelling time with increasing *N*-iPAAm/PEGMEMA ratio. This indicates that hydrogen bond arrangements between MAA and *N*-iPAAm are stronger that those formed by MAA and PEGMEMA. The influence of the polymer composition on the hydrogen bond arrangements was also studied from the swelling kinetics curves at different pH media, observing that the swelling rate, the swelling curve shape and the whole amount of water absorbed were clearly dependent on this parameter.

1. Introduction

Stimuli-responsive hydrogels are characterized by undergoing relatively large and abrupt, physical or chemical changes in response to external variations in the environmental conditions. These stimuli can be classified as either physical (temperature, magnetic fields, mechanical stress, etc.) or chemical (pH, ionic strength, etc.). This behaviour is very useful in applications such as drug delivery [1–5], biotechnology [3,6,7] or chromatography [6,8–10]. Furthermore, some polymer systems have been developed to combine two or more stimuli-responsive mechanisms. For instance, temperature-sensitive polymers may also respond to pH changes [11–14].

In recent years, poly(*N*-isopropylacrylamide-*co*-methacrylic acid), P(*N*-iPAAm-*co*-MAA), copolymers have been studied as one of these temperature and pH sensitive materials [15–26]. These copolymers show different properties depending on composition and previous swelling treatment [22,23,25], which potentially allows obtaining hydrogels for specific uses. Thus, copolymers with a high *N*-iPAAm content are able to respond to temperature changes at low pH, whereas the ionizable carboxyl group of the MAA moiety furnishes pH-sensitivity for the whole range of copolymer composition. In addition, these copolymer hydrogels exhibit strong interactions among their comonomeric units. Hydrogen bond arrangements between carboxylic groups of MAA units and amide groups of *N*-iPAAm units have been detected [24,27]. These bondings occur at pH below the pK_a of MAA, and they disrupt at neutral and high values of pH with a slow swelling rate. Therefore, anomalous behaviour was found in the swelling experiments, which was explained by the reversible character of the hydrogen bonds when the pH of the medium is changed [22,23]. On one hand, it has been found that swelling curves for some of these copolymers hydrogels at pH 7 exhibit sigmoidal shapes. This fact was related to the limited rate of the hydrogen bond disruption between both comonomeric units during swelling, following autocatalytic kinetics. On the other hand, swelling curves in acidic media exhibit an overshoot, which has been attributed to a swelling–deswelling process due to hydrogen bond formation during swelling [28]. The shape of the swelling curve was found to

* Corresponding author. Tel.: +34 91 258 74 30/562 29 00; fax: +34 91 564 48 53.
E-mail address: iquijada@ictp.csic.es (I. Quijada-Garrido).

0032-3861/$ – see front matter © 2009 Elsevier Ltd. All rights reserved.
doi:10.1016/j.polymer.2009.02.028

Table 1
Diffusion exponents and rate constants obtained by fitting to Eq. (2) the swelling data of the P(*N*-iPAAm-*co*-MAA-*co*-PEGMEMA) terpolymeric hydrogels (pH 7 and 25 °C). In all syntheses $[MAA]_0 = 50$ mol% $[APS]_0 = [TEGDMA]_0 = [TEMED]_0 = 0.50\%$ (w/w). Solvent [water/ethanol = 1/1(v/v)] = 50% (w/w).

Sample	Feed Composition (mol%)		Estimated composition (mol%)		n	$k \times 10^3$ (min^{-1})	R^2
	N-iPAAm	PEGMEMA[a]	*N*-iPAAm[b]	PEGMEMA[a,c]			
1	50	0	50.7	–	0.87	3.4	0.997
2	40	10	43.8	11.0	0.84	4.8	0.997
3	30	20	34.5	17.8	0.80	5.7	0.997
4	20	30	26.7	23.8	0.70	12.2	0.995
5	10	40	15.4	34.0	0.78	6.2	0.998
6	0	50	–	49.4	0.77	6.1	0.999

[a] Related to the $[OCH_2CH_2]$ units.
[b] Determined by elemental analysis.
[c] Determined by ^{13}C CP-MAS NMR.

depend on the previous swelling history, namely the previous soaking pH in which the hydrogels have been submitted [22,28].

Our research group has also studied another type of pH-sensitive hydrogel in which interactions between comonomers are present, such as those based on MAA and poly(ethylene glycol) monomethyl ether monomethacrylate macromonomer (PEGMEMA) [29]. These P(MAA-*co*-PEGMEMA) hydrogels offer some special peculiarities in addition to the biocompatibility and excellent physicochemical properties of poly(ethylene glycol). They can respond to the surrounding pH by the formation of polymer complexes due to hydrogen bond interactions between the –COOH groups of the MAA in the main chain and the $[-O-CH_2-CH_2-]$ groups of the poly(ethylene glycol) monomethyl ether side chains. More specifically, at low pH, the hydrogen bonds between ether and carboxyl groups promote polymer collapse whereas, at high pH, carboxylic groups ionize and the polymer swells and behaves as a polyelectrolyte. In these systems an autocatalytic swelling behaviour was newly found, which depends on sample composition because it is related to the hydrogen bond arrangements between both comonomeric units. Therefore, the autocatalytic process was more remarkable for copolymer with equimolecular $[-COOH]/[-O-CH_2-CH_2-]$ ratio. The swelling behaviour of both hydrogel systems described in this introduction was determined gravimetrically. Nevertheless, they were also studied by magnetic resonance imaging (MRI) [26,29], this technique is quite interesting because it provides a spatial and a temporal resolution of the swelling process. MRI has been used widely to monitor the diffusion of water and other solvents into synthetic polymers [30]. It is a non-invasive imaging system which has found widespread application in hydrogels to monitor the change in water uptake with time, thus allowing the study of swelling and water diffusion in real time [31–35].

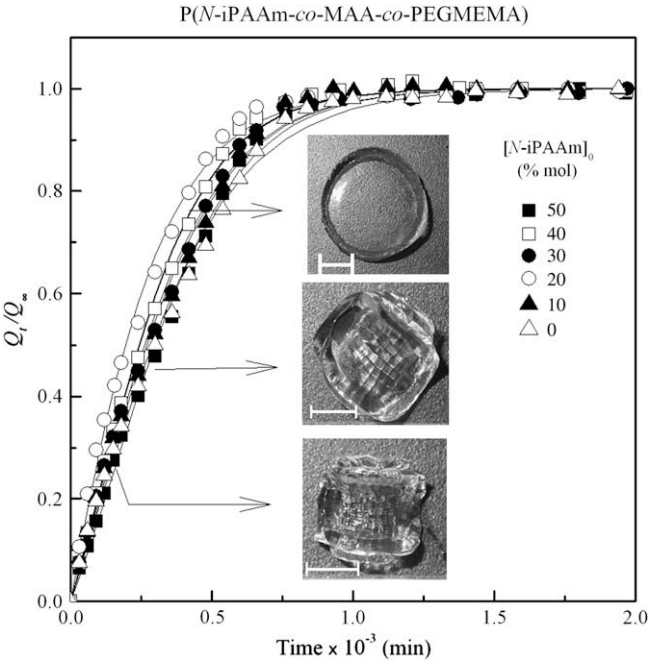

Fig. 1. Normalized gravimetric swelling isotherms in water at pH 7 and 25 °C for a series of P(*N*-iPAAm-*co*-MAA-*co*-PEGMEMA) random terpolymeric hydrogels ($[MAA]_0 = 50\%$). Photographs taken at different stages of swelling for the sample with $[N\text{-iPAAm}]_0 = 10$ mol% are also represented, in which the scale bar represents 0.5 cm.

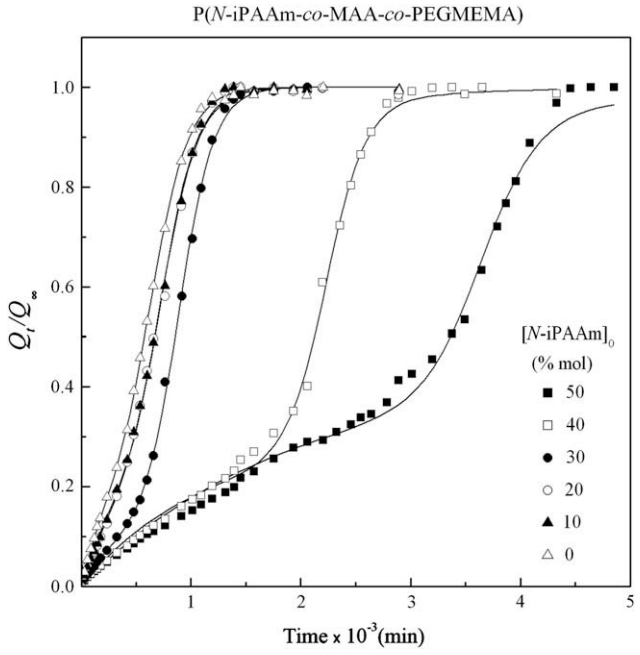

Fig. 2. Normalized gravimetric swelling isotherms in water at pH 7 and 25 °C for a series of P(*N*-iPAAm-*co*-MAA-*co*-PEGMEMA) random terpolymeric hydrogels previously soaked in pH 2 solution.

The main aim of this work is to study the dynamic swelling behaviour of new hydrogels based on terpolymers of *N*-iPAAm, MAA and PEGMEMA, P(MAA-*co*-*N*-iPAAm-*co*-PEGMEMA) in order to modulate the swelling rate at pH 7. A slow and sustainable swelling is useful in applications such as drug controlled release. Systems based on MAA with either *N*-iPAAm or PEGMEMA showed a hydrogen bond dependent swelling behaviour. For this reason, it is logical to think that these terpolymeric hydrogels are going to present different chemical interactions and therefore, different

Table 2
Swelling parameters (pH 7 and 25 °C) of the P(*N*-iPAAm-*co*-MAA-*co*-PEGMEMA) terpolymeric hydrogels. k_1 and k_2 were obtained by fitting the data to Eq. (3). In all syntheses $[MAA]_0 = 50$ mol% $[APS]_0 = [TEGDMA]_0 = [TEMED]_0 = 0.50\%$ (w/w). Solvent [water/ethanol = 1/1(v/v)] = 50% (w/w).

Sample	$t_{1/2}$ (min)	Q_∞	$k_1 \times 10^3$ (min^{-1})	$k_2 \times 10^3$ (min^{-1})	R^2
1	319	32.1	1.52	3.20	0.997
2	255	30.7	2.04	3.13	0.997
3	281	32.5	2.00	2.53	0.997
4	198	34.3	3.14	1.55	0.997
5	272	31.7	1.89	2.66	0.995
6	292	33.5	1.85	2.12	0.996

Table 3
Swelling parameters (pH 7 and 25 °C) of the P(*N*-iPAAm-*co*-MAA-*co*-PEGMEMA) terpolymeric hydrogels pre-soaked in pH 2 solution. k_1, k_2, k_3 and β were obtained by fitting the data to Eq. (3). In all syntheses $[MAA]_0 = 50$ mol% $[APS]_0 = [TEGDMA]_0 = [TEMED]_0 = 0.50\%$ (w/w). Solvent [water/ethanol = 1/1 (v/v)] = 50% (w/w).

Sample	pH medium	$t_{1/2}$ (min)	Q_∞	$k_1 \times 10^5$ (min^{-1})	$k_2 \times 10^3$ (min^{-1})	$k_3 \times 10^3$ (min^{-1})	β	R^2
1	7	3341	31.4	<1	3.6	0.58	0.398	0.995
2	7	2065	30.9	<1	5.6	0.94	0.293	0.999
3	5	–	–	3	0.3	–	–	0.999
	7	830	32.6	2	6.2	3.57	0.107	0.999
	9	916	35.3	1	6.6	2.31	0.221	0.999
4	5	–	–	5	0.3	–	–	0.998
	7	647	34.9	8	5.7	3.30	0.186	0.999
	9	602	35.1	1	10.6	3.27	0.278	0.999
5	7	640	32.4	7	6.0	3.21	0.209	0.999
6	7	552	34.7	15	5.6	5.21	0.165	0.999

swelling behaviours depending on composition, pH medium and previous swelling treatment. Their syntheses were performed employing a constant MAA ratio (50 mol%) because in both copolymeric systems the most favourable interactions were found for equimolecular compositions [22,23,25,29] and also, varying systematically the molar ratio of *N*-iPAAm and PEGMEMA (respect to [–O–CH_2–CH_2–] content) in order to analyze the compositional effect. Gravimetric, photographic and MRI techniques will be used to elucidate the swelling behaviour.

2. Experimental section

2.1. Materials

The monomer *N*-isopropylacrylamide (*N*-iPAAm, Acros Organics 99%) was purified by recrystallization from *n*-hexane/toluene mixture (90/10 v/v). The other two monomers, methacrylic acid (MAA) (Fluka 98%) and poly(ethylene glycol) monomethyl ether monomethacrylate macromonomer (PEGMEMA) ($\overline{M}_n \sim 2080$ Da, Aldrich, 50% solution in water) were employed without any previous purification. The crosslinker tetraethylene glycol dimethyl acrylate (TEGDMA) (Fluka ≥90%), the activator *N*,*N*,*N*′,*N*′-tetramethylethylenediamine (TEMED) (Fluka ≥99%), the initiator ammonium persulfate (APS) (Fluka ≥98%) and sodium hydroxide (Panreac ≥98%) were used as-received. Solvents ethanol (Normapur, A.R.), *n*-hexane (Panreac 98%) and toluene (Merck 99.7%) were also employed as-received. Water for all reactions, buffer solutions for swelling experiments and hydrogel purification were Milli Q from water purification facility (Millipore Milli-U10). Phosphate buffer solutions (PBS) were prepared employing sodium dihydrogen phosphate anhydrous (Fluka ≥99%), disodium hydrogen phosphate (Panreac ≥98%), ortho phosphoric acid (Panreac 85%) and sodium chloride (Panreac ≥99.5%) in order to keep constant the ionic strength (0.1 M). Gadopentetate dimeglumine (Gd-DTPA, Shering AG) was used to reduce the spin-lattice relaxation time, T_1, of water protons in MRI experiments.

2.2. Syntheses of P(N-iPAAm-co-MAA-co-PEGMEMA) terpolymers

P(*N*-iPAAm-*co*-MAA-*co*-PEGMEMA) hydrogels were synthesized by free-radical cross-linking random polymerization in solution of the three monomers. Six different polymers were obtained employing the monomer feed percentages described in Table 1. Polymerizations were carried out using a mixture of water and ethanol (50/50 v/v) as solvent. In all cases the monomers/solvent ratio was 1:1 (w/w), being the MAA monomer neutralized by means of an aqueous NaOH solution (2 N). Crosslinker TEGDMA, activator TEMED, and initiator APS were used with an initial weight ratio of 0.5% of the total monomer amount.

The procedure to obtain sheet shaped gels was as follows: the mixture solution was cast on glass plates enclosed by a rubber framework-spacer with 1 mm thickness and sealed off with other glass plate in order to avoid air contact during the polymerization (24 h). Afterward, the gel sheets were removed from the glass plate and immersed in freshwater for, at least, 3 days to remove the unreacted chemicals. During this time, water was replaced several times. After that, the gels were dried at room temperature and then, they were swollen in water at a gel/solvent ratio of 1:1 (w/w) until equilibrium. Thus, uniform disks of 6 mm diameter were punched out the gel sheet using a stainless steel cork borer. These disks were left to dry at room temperature for 48 h. Additionally, since the previous swelling treatment was shown to have a strong influence on the swelling behaviour [22], samples were soaked in acid medium (pH 2) for 48 h and then, dried at room temperature until constant weight.

2.3. Estimation of terpolymer composition

N-iPAAm content of each copolymer was estimated by organic elemental analysis. MAA and PEGMEMA contents were estimated by ^{13}C CP-MAS NMR on a Bruker Avance 400 spectrometer/imager (Bruker Analytik GmbH, Karlsruhe, Germany) equipped with a Bruker UltraShield 9.4 T (^1H resonance frequency of 400.14 MHz). The 90° pulse lengths were 5.3 and 3.3 μs for ^{13}C and ^1H, respectively. ^{13}C CP-MAS spectra were measured with 1 ms contact time,

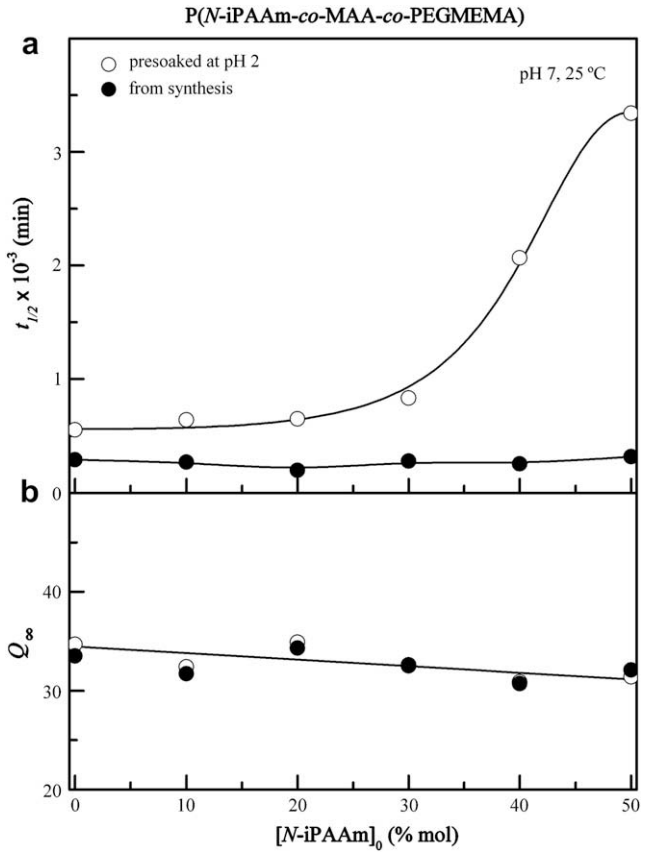

Fig. 3. (a) Time at half of swelling and (b) swelling equilibrium values as a function of $[N\text{-iPAAm}]_0$ content.

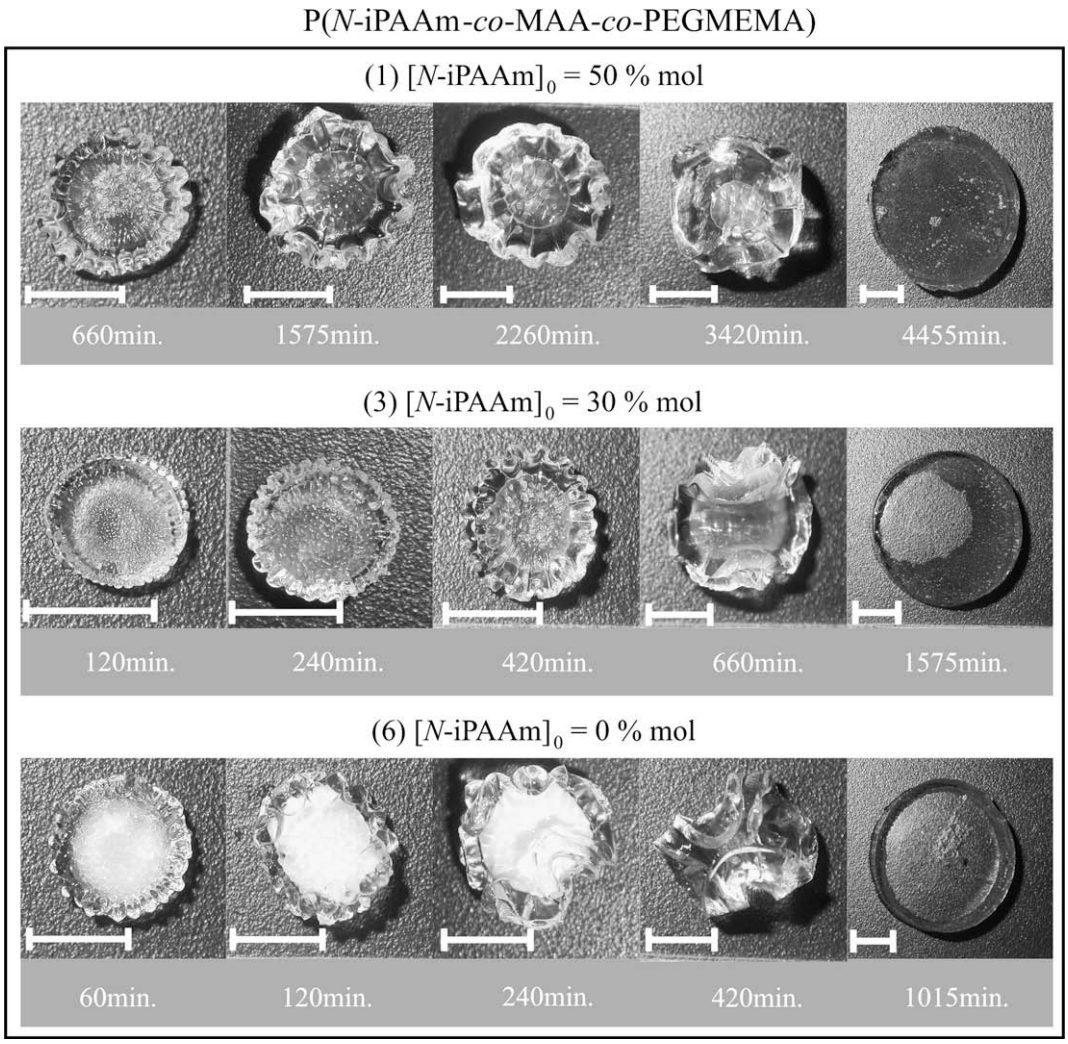

Fig. 4. Photographs taken at different stages of swelling for a series of disk-shaped P(*N*-iPAAm-*co*-MAA-*co*-PEGMEMA) random terpolymers with different composition previously soaked in pH 2 solution. The scale bar represents 0.5 cm.

30 kHz spectral width and up to 5000 scans. Sample was spun at frequencies of 7 kHz. The chemical shifts ^{13}C spectra were referenced to tetramethylsilane (TMS) by using adamantante as secondary standard. Resulting compositions are collected in Table 1.

2.4. Gravimetry of the hydrogels during swelling

Dried pre-soaked disks were left to swell in PBS at the selected pH (ionic strength = 0.1 M) at 25 °C. After regular time intervals, samples were taken out, wiped superficially with blotting paper, weighed, photographed and placed again in the same bath. The swelling ratio or degree of swelling, Q_t, at a time t was calculated in weight of water per weight of dry gel (xerogel) using the following expression:

$$Q_t = (m_t - m_0)/m_0 = W_t/m_0 \quad (1)$$

where m_t is the weight of the swollen gel at time t, m_0 is the weight of the xerogel, and W_t is the water uptake at time t. The normalized swelling rate is obtained by the relation Q_t/Q_∞, where Q_∞ is the degree of swelling at equilibrium. Moreover, the swelling curves were performed by duplicate in order to assure the accuracy of the results.

2.5. Photography of the hydrogels during swelling

Photographs of the hydrogel disks were recordered with a Nikon digital camera COOLPIX 4500 at regular intervals during swelling experiments.

2.6. Magnetic resonance imaging (MRI)

All ^1H MRI experiments were also carried out on a Bruker Avance 400 spectrometer/imager. The NMR images were acquired at room temperature by using a standard Bruker imaging probe with a 25 mm diameter rf insert. A standard Bruker 2D spin echo pulse sequence was used to acquire the data which were converted into proton density maps using Paravision software supplied with the spectrometer. An echo time TE of 4.393 ms and a repetition time TR of 1 s were used. Four scans were averaged for each image with a field of view (FOV) of 25 × 25 mm and a slice thickness of 0.25 mm. For each image a non-isotropic matrix of 256 × 128 pixels with a spatial resolution of 98 × 195 μm was acquired. To keep the sample at the same spatial position during the experiment, each hydrogel disk was supported on a polyethylene net with a nylon filament crossing its centre, in a similar way as it has been shown elsewhere [26].

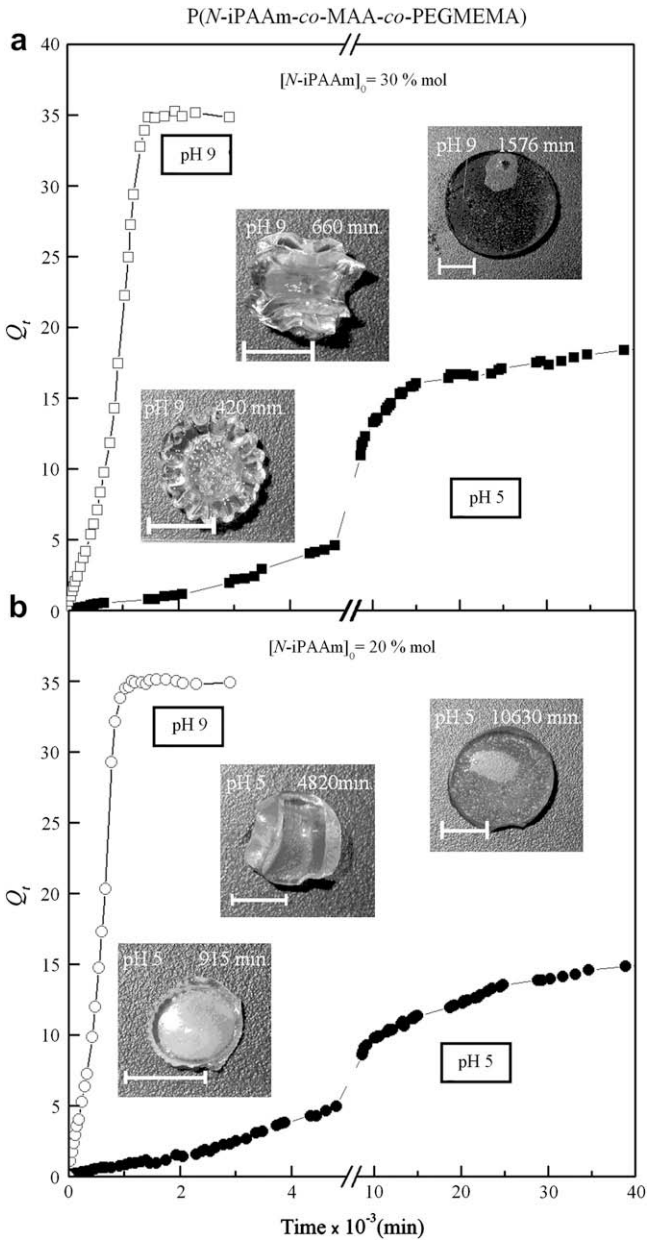

Fig. 5. Gravimetric swelling isotherms in water at pH 5 and 9 at 25 °C for samples (a) 3 and (b) 4 of P(*N*-iPAAm-*co*-MAA-*co*-PEGMEMA) random terpolymeric hydrogel pre-soaked in pH 2 solution. Time-dependent photographs taken at different stages of swelling have been also included. The scale bar represents 0.5 cm.

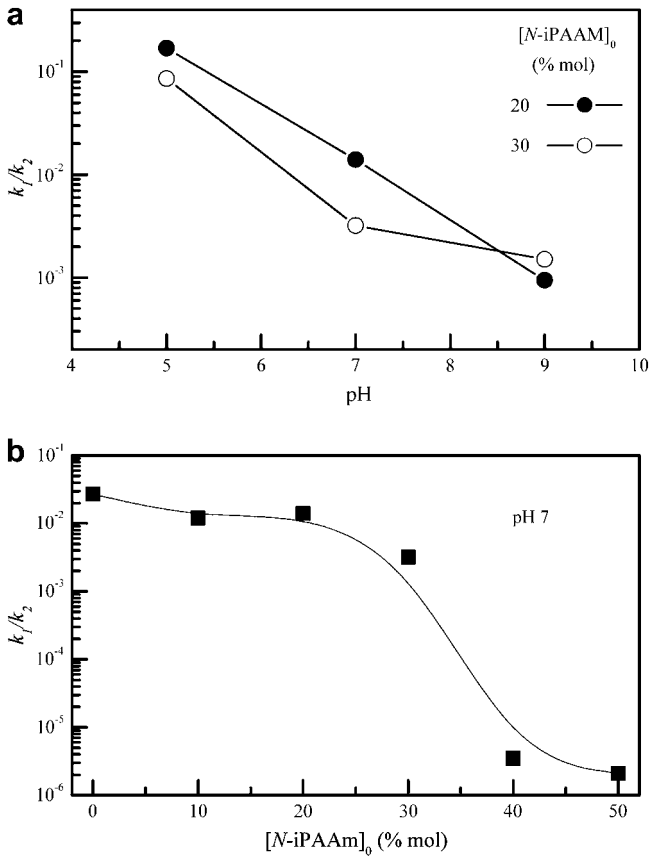

Fig. 6. k_1/k_2 ratio as a function of (a) $[N\text{-iPAAm}]_0$ and (b) pH medium for the terpolymers with 20 and 30 mol% of $[N\text{-iPAAm}]_0$ content.

3. Results and discussion

3.1. Macroscopic swelling experiments: gravimetric and photographic analyses

Dynamic gravimetric swelling curves at pH 7 of the P(*N*-iPAAm-*co*-MAA-*co*-PEGMEMA) hydrogels without previous pH treatment are shown in Fig. 1, where photographs of the disk samples corresponding to the sample with $[N\text{-iPAAm}]_0 = 10$ mol% at different stages of swelling have also been included. The shapes of these curves were almost independent on hydrogel composition. Therefore, from a classic approximation, the water diffusion mechanism can be characterized analyzing the sorption profile, Q_t/Q_∞, versus time curves by using the following equation [36]:

$$\frac{Q_t}{Q_\infty} = kt^n \tag{2}$$

where k is a constant incorporating the characteristics of the macromolecular network system and the penetrant. The parameter n is the diffusional exponent, which has been used as an indicator of the diffusion mechanism. Thus, for Case I (Fickian) diffusion, $n = 0.5$, while for Case II, $n = 1$, and for Super Case II, $n > 1$.

The fitting of the experimental results to Eq. (2), for $Q_t/Q_\infty < 0.6$, leads to the values of n and k for each sample collected in Table 1. The values of n vary from 0.7 to 0.9, which may indicate that swelling is controlled by a non-Fickian mechanism. This is not surprising since these systems establish physical interactions, which depend on the pH.

Fig. 2 shows the swelling curves under pH 7 for the same samples but previously soaked in pH 2 solution in order to favour the formation of hydrogen bond bridges between comonomeric units. Comparing this Fig. 2 with Fig. 1, the strong effect of the previous swelling treatment can be observed, presenting the swelling curves sigmoidal shapes for the whole range of composition. Sigmoidal swelling curves for water uptaking may be found in the literature for some other systems [37–42]. Thus, Siegel et al. [37–39] and Falamarzian et al. [40] found this anomalous behavior for hydrophobic weak base polyelectrolyte copolymers of methyl methacrylate (MAA) and *N*,*N*-dimethylamino methacrylate (DMA), when they swell under acidic media. On the other hand, Okano and co-workers [41,42] found sigmoidal swelling curves for thermoresponsive hydrogels of poly[(*N*-iPAAm)-*co*-(*n*-butyl methacrylate)], a neutral hydrophobic hydrogel. It is our belief that the sigmoidal

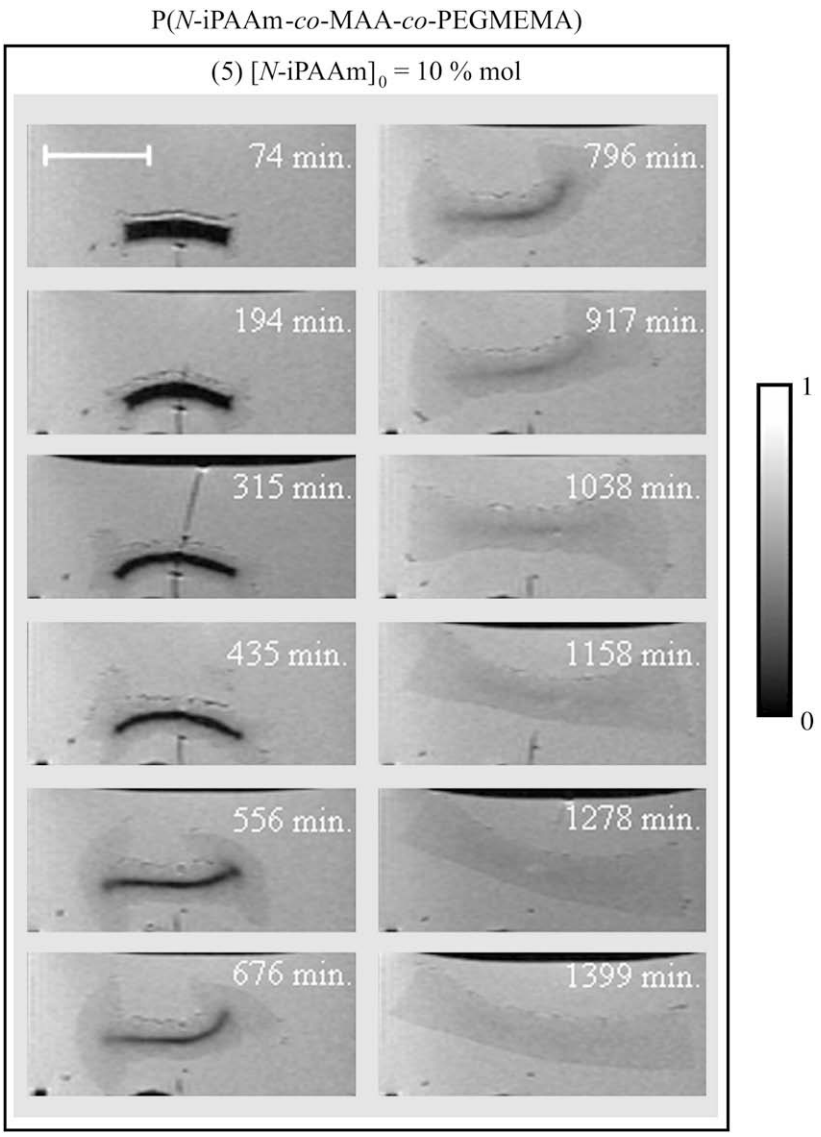

Fig. 7. Proton MRI images corresponding to the swelling of the sample 5 of P(*N*-iPAAm-*co*-MAA-*co*-PEGMEMA) random terpolymer pre-soaked in pH 2 solution. The scale bar represents 0.5 cm.

behavior in the case of P(*N*-iPAAm-*co*-MAA-*co*-PEGMEMA) obeys to the fact that in these cases the hydrogen bonds are more inaccessible to water molecules since they are stabilized by hydrophobic interactions.

This experimental sigmoidal swelling profile was analyzed previously by our research group according to an autocatalytic mechanism, suggesting that cooperativity of hydrogen bond breaking controls the swelling behaviour [26,29]. Hydrogen bond arrangements formed at low pH between MAA and the others two monomers restrict the incorporation of water molecules. On one hand, this physical crosslinking decreases the mobility of the network and, on the other hand, because hydrogen bonds are stabilized by hydrophobic forces. Therefore, the swelling behaviour is controlled by the kind and amount of hydrogen bonds formed, apart from the control of the diffusion process, typical of these hydrogels systems. Coming back to Fig. 2, it is observed that swelling rate decreases as the *N*-iPAAm content increases. We assume that it is a consequence of the higher strength of MAA/*N*-iPAAm hydrogen bonds arrangements compared to those formed by MAA and the ethylene glycol units in the side chains.

From an analytical point of view, this swelling process may be represented by the following equation:

$$Q_t/Q_\infty = \beta\left(1 - e^{-k_3 t}\right) + (1-\beta)(k_1/k_2)\left(1 - e^{-(k_1+k_2)t}\right)\Big/\left((k_1/k_2) + e^{-(k_1+k_2)t}\right) \quad (3)$$

where the first term represents the advance of the swelling front, and the second one, the autocatalytic contribution to the swelling. β is the fraction of each one of both contributions to the overall process. The ratio between the two rate constants, k_1 and k_2, controls the shape of the curve. Thus, when $k_1 >> k_2$, $(k_1 + k_2) \approx k_1$, and therefore $(k_1 + k_2) \gg e^{-(k_1+k_2)}$, Eq. (3) becomes to a first-order process: $Q_t/Q_\infty = (1 - e)^{-k_1 t}$, where k_1 would be a true first-order rate constant. When $k_1 << k_2$ the swelling curve presents a sigmoidal shape and k_1 is related to the lag time.

Tables 2 and 3 show the values of the swelling parameters, the kinetic constants and the determination coefficients (R^2) from the fitting of the experimental swelling curves of samples without and with previous acid treatment to Eq. (3), respectively. Moreover,

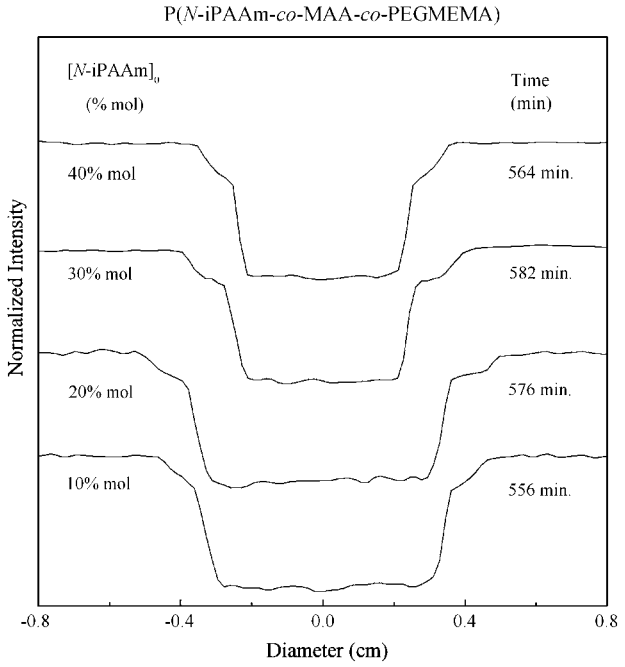

Fig. 8. One-dimensional spin density profiles extracted from the MRI experiments, at the times shown, for a series of P(*N*-iPAAm-*co*-MAA-*co*-PEGMEMA) random terpolymer pre-soaked in pH 2 solution.

simulated curves with parameters from the fittings are also shown as solid lines in the respective figures. In the case of the samples without any previous treatment, the first exponential term is not necessary to obtain a good fit. This means that from the beginning, water can access to the hydrogel core and only the autocatalytic process is significant. In addition, the estimated constant rate values are in agreement with those previously determined for similar systems [22,29]. In Fig. 3a, the time at half of swelling ($t_{1/2}$) for the whole range of hydrogels investigated is presented as a function of monomeric composition. For samples pre-soaked in pH 2 solution, $t_{1/2}$ is higher compared to samples that were not pre-soaked. Furthermore, $t_{1/2}$ remains almost constant for enriched PEGMEMA hydrogels and increases rapidly when $[N\text{-iPAAm}]_0$ content exceeds 30 mol%. Fig. 3b shows the values of the degree of swelling at equilibrium, Q_∞, versus the $[N\text{-iPAAm}]_0$ content for both swelling pre-treatments. As it was expected, this value is independent on the swelling pre-treatment. It is also interesting that Q_∞ does not appreciably depend on monomeric composition.

Photographs, taken at different stages of swelling, from P(*N*-iPAAm-*co*-MAA-*co*-PEGMEMA) hydrogel slabs are shown in Fig. 4 for the samples pre-soaked in acidic pH solution. The hydrogel disks present a complex morphology. As a general behaviour, in the intermediate step, disks display a scalloped pattern on the surface and edges, corresponding to the development of a swelling front with higher water content than the core. The core zone is transparent at the beginning, when is dried. However, until a certain time, which depends on composition, it becomes opaque. This fact indicates phase separation. In a second step, the core began to swell quickly and the disks become transparent and show regular shapes. This behaviour has been attributed to an anisotropic swelling of the samples, as it will be supported by the MRI experiments in the next section.

In order to carry out a further analyze on the pH effect, the swelling behaviour of samples 3 and 4, pre-soaked in pH 2 solution, was studied under pH 9 and 5. These results are displayed in Fig. 5. At pH 9, the swelling curves were almost similar to those obtained at pH 7 (see Fig. 2), just showing a slightly increase of the swelling rate, especially for the sample with the higher PEGMEMA content

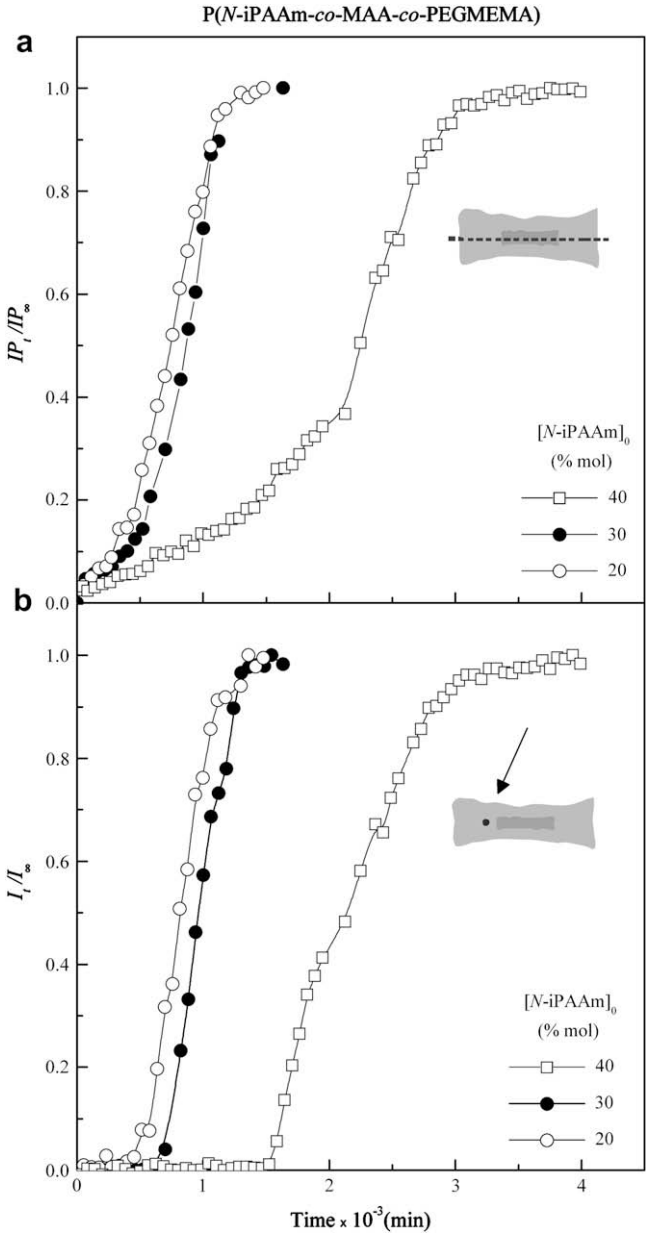

Fig. 9. Swelling curves at pH 7 and 25 °C obtained from MRI images of P(*N*-iPAAm-*co*-MAA-*co*-PEGMEMA) terpolymers pre-soaked in pH 2 solution. (a) Normalized integral of the spin density profiles measured along a line crossing the hydrogels along its longer direction, IP_t/IP_∞, versus time. (b) Normalized integral of the spin density profiles measured at a point indicated in this figure I_t/I_∞.

(swelling parameters shown in Table 3). This fact has been related to the lower stability of the hydrogen bonds formed in this case. At pH 5, which is closer to the pK_a of MAA, the swelling behaviour is clearly different; indicating again that the swelling behaviour of these terpolymers is strongly dependent on the pH of the medium. Two main differences are observed: (i) the swelling rate is remarkably slow and, (ii) the equilibrium swelling is not immediately reached after acceleration, where the swelling degree increases slowly and almost linearly. This fact could be attributed to the existence of hydrogen bonds that are not disrupted in the autocatalytic process, but they are not in equilibrium at this pH.

As it was explained above, the balance between the two rate constants, k_1 and k_2, controls the shape of the swelling curves. Thus, the experimental variations of k_1/k_2 as function of the pH medium and also as function of the feed monomeric composition are plotted

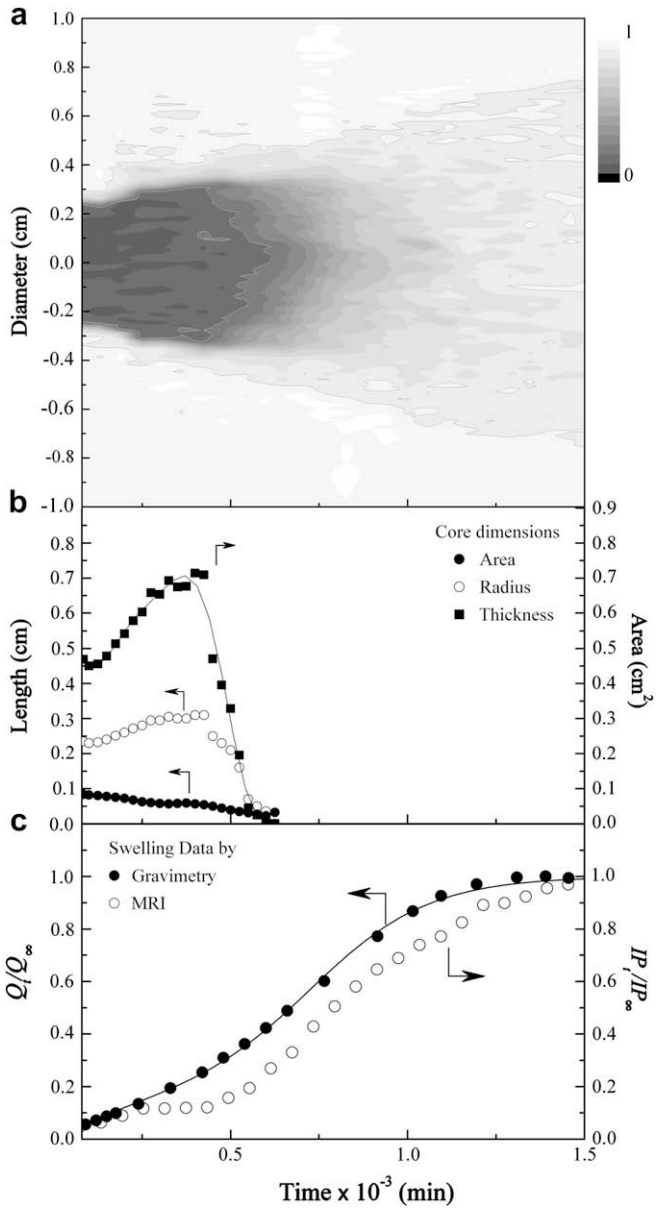

Fig. 10. (a) Contour map representing the spin density profile, for the sample 5 of P(*N*-iPAAm-*co*-MAA-*co*-PEGMEMA) terpolymer at pH 7 and 25 °C, pre-soaked in pH 2 solution, as a function of swelling time. (b) Evolution of the core diameter, core thickness and core area. (c) Evolution of the swelling by gravimetric and MRI experiments.

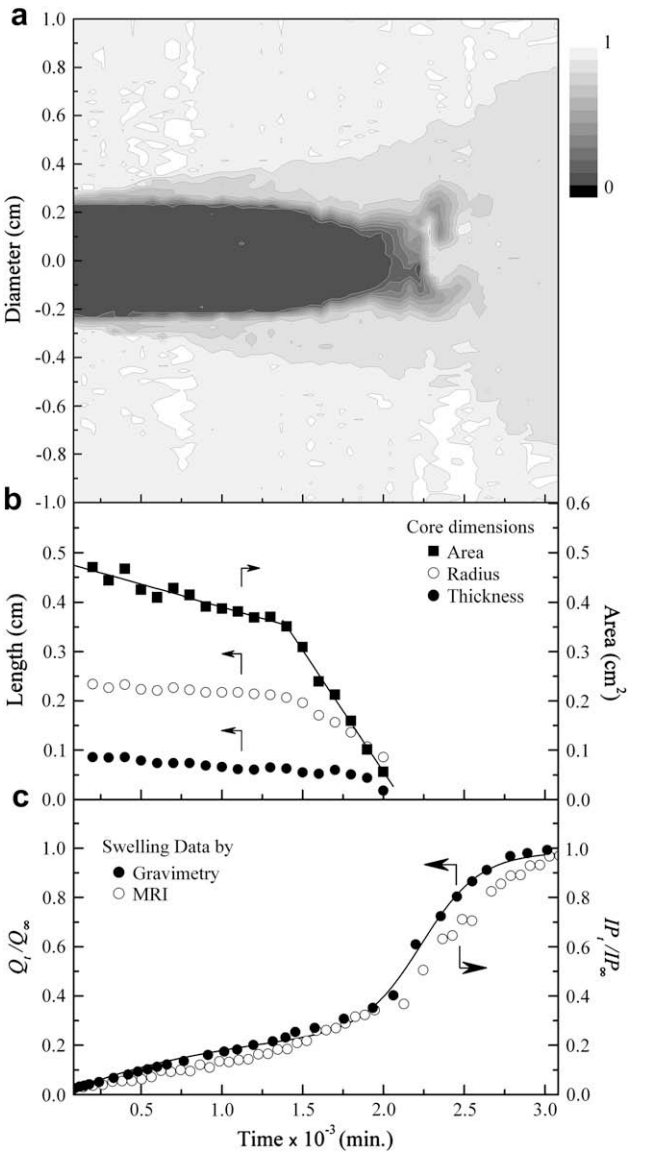

Fig. 11. (a) Contour map representing the spin density profile, for the sample 2 of P(*N*-iPAAm-*co*-MAA-*co*-PEGMEMA) terpolymer at pH 7 and 25 °C, pre-soaked in pH 2 solution, as a function of swelling time. (b) Evolution of the core diameter, core thickness and core area. (c) Evolution of the swelling by gravimetric and MRI experiments.

in Fig. 6 for samples pre-soaked in pH 2 solution. In general k_1 is much lower than k_2, indicating a marked acceleration of the process. In addition, the k_1/k_2 ratio decreases when both, pH medium and *N*-iPAAm content increase. The lowest k_1/k_2 ratio is obtained for the samples with the highest *N*-iPAAm content, according with the swelling curves. In addition, k_3 decreases with increasing *N*-iPAAm content (see Table 3), which means that the advance of the swelling front is lower for these samples, indicating again the higher strength and cooperativity of *N*-iPAAm/MAA hydrogen bond arrangements.

3.2. Swelling monitorization by magnetic resonance imaging (MRI)

According to our previous works [26,29], the swelling behaviour at pH 7 of the P(*N*-iPAAm-*co*-MAA-*co*-PEGMEMA) random terpolymers pre-soaked in pH 2 solution was analyzed by MRI in order to evaluate the water distribution inside the gel at real time. As an example, Fig. 7 shows ^{1}H NMR images corresponding to different stages of swelling for sample 5 ($[N\text{-iPAAm}]_0 = 10$ mol%). False grey-scale represents the relative proton signal intensity. The most mobile region, corresponding to the water outside the gel, gives the highest intensity, whereas rigid regions from the non-hydrated gel are seen darker. A common fact observed in all hydrogels is the presence of a core which remains almost unswollen during a first stage. To illustrate this effect, one-dimensional proton intensity profile, which corresponds to the proton intensity of a line crossing the hydrogels along its longer direction in the middle plane, is presented in Fig. 8 for each terpolymer at a similar swelling time. Two parts appear in all the samples; a core which shows much lower intensity that the outer part where the mobility of the water is higher. After this first step,

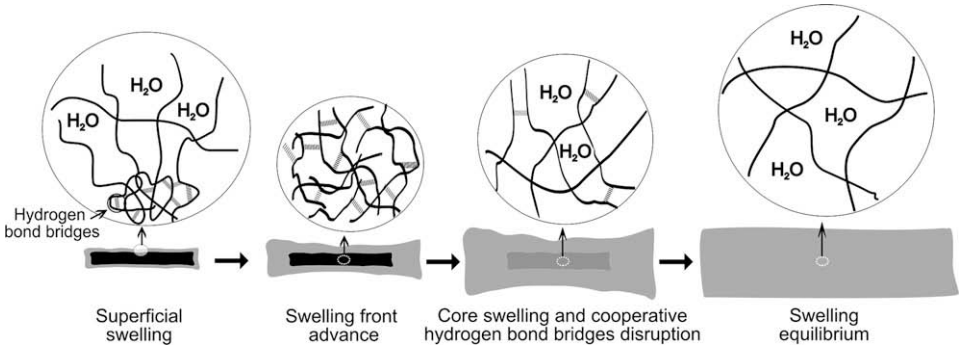

Scheme 1. Swelling stages of hydrogen bonded hydrogels.

the core starts to swell rapidly, giving place to the accelerating effect observed in the gravimetric analysis shown in Fig. 2.

In addition, from the normalized integral of the MRI signal intensity profiles at each time (IP_t/IP_∞), a curve related to the swelling process for each terpolymer has been obtained. They are colleted in Fig. 9a. The curves have similar trend as those ones obtained from the gravimetric experiments. Furthermore, Fig. 9b shows the evolution of the normalized signal intensity at a point (I_t/I_∞), namely in between the centre of the sample and its edges. At this point, it is observed the existence of a delay time in the swelling process of the terpolymers. After this time the swelling occurs in almost an exponential fashion. This means that the core is not hydrated until a certain induction time, which depends on the hydrogen bonds formed in each sample.

Taken water intensity profiles as function of time, intensity contour maps may be obtained, which are very useful to study the water distribution in the hydrogel and its change with time. Thus, Figs. 10 and 11 show contour maps corresponding to samples with 10 and 40% mol of [*N*-iPAAm]$_0$, respectively. The swelling curves have also been included. In both cases, the acceleration of the swelling curves agree with the increase of the intensity (water mobility) in the core. However, differences are observed comparing these two samples: thus, whereas in the sample with the higher *N*-iPAAm content the core remains dry a long time, in the sample with higher PEGMEMA content, a small amount of water penetrates rapidly to the core, observing a little increase of the core diameter before the acceleration starts. On the contrary, from Fig. 11b, it may be also observed that, in the sample with the higher *N*-iPAAm content, the core dimensions decrease very slowly and almost linearly with the swelling time. This fact reveals that enriched *N*-iPAAm terpolymers should present higher hydrophobicity that enriched PEGMEMA ones. Other interesting fact that can be derived from the MRI experiments is that swelling takes place faster in the radial than in the thickness direction. This could be because the swollen parts have more place to expand in the radial direction.

The swelling process in these terpolymers occurs as is summarized in Scheme 1: (a) in a first step, swelling takes place only on the exposed surface, (b) the swelling front advances to the centre of the sample but, in the core, the hydrogen bonded structure remains, (c) water penetrates to the core and starts to disrupt the hydrogen bond arrangements, producing the acceleration profile in the swelling and (d) the physical crosslinking disappears and a swelling equilibrium is achieved.

4. Conclusions

New pH-responsive stimuli hydrogels of MAA (50% mol) with *N*-iPAAm and PEGMEMA in different proportions, P(*N*-iPAAm-*co*-MAA-*co*-PEGMEMA) terpolymers, were synthesized. From the experimental results of their swelling behaviour as a function of monomer composition, pH and previous swelling treatment, the following conclusions can be drawn: (i) the swelling behaviour clearly depends on the capability of the samples to form hydrogen bonds arrangements. Thus, the swelling at pH 7 of samples pre-soaked in pH 2 solution, establishes a kinetic shape characterized by an induction time followed by an autoacceleration process. (ii) The kinetic swelling curves were markedly influenced by the monomer composition in the samples treated at low pH. The *N*-iPAAm/PEGMEMA ratio determined the number and strength of the hydrogen bonds with MAA and therefore, the rate and shape of the swelling process. (iii) These processes were also dependent on the pH of the swelling medium. pH affects the ionization of the acid group in MAA monomer and therefore, to the number of hydrogen bonds bridges. (iv) MRI experiments indicate that samples with higher *N*-iPAAm content exhibit hydrogen bond arrangements of higher stability.

Acknowledgments

This work was financially supported by the Consejo Superior de Investigaciones Científicas (C.S.I.C.). The authors also acknowledge the financial support provided by the Ministerio de Ciencia e Innovación (CTQ2008-03229) by the Comunidad Autónoma de Madrid (CAM S0505/MAT/0227) and by de Ministerio de Sanidad y Consumo (FIS PI05/1847). I.Q.-G. thanks the CSIC for a PIE project (200760I024).

References

[1] Chilkoti A, Dreher MR, Meyer DE, Raucher D. Adv Drug Deliv Rev 2002;54(5):613–30.
[2] Gupta P, Vermani K, Garg S. Drug Discov Today 2002;7(10):569–79.
[3] Jeong B, Gutowska A. Trends Biotechnol 2002;20(7):305–11.
[4] Qiu Y, Park K. Adv Drug Deliv Rev 2001;53(3):321–39.
[5] Sershen S, West J. Adv Drug Deliv Rev 2002;54(9):1225–35.
[6] Galaev IY, Mattiasson B. Trends Biotechnol 1999;17(8):335–40.
[7] Sharma S, Kaur P, Jain A, Rajeswari MR, Gupta MN. Biomacromolecules 2003;4(2):330–6.
[8] Anastase-Ravion S, Ding Z, Pelle A, Hoffman AS, Letourneur D. J Chromatogr B Biomed Sci Appl 2001;761(2):247–54.
[9] Kobayashi J, Kikuchi A, Sakai K, Okano T. J Chromatogr A 2002;958(1–2):109–19.
[10] Kikuchi A, Okano T. Prog Polym Sci 2002;27(6):1165–93.
[11] Bignotti F, Penco M, Sartore L, Peroni I, Mendichi R, Casolaro M, et al. Polymer 2000;41(23):8247–56.
[12] Gan LH, Gan YY, Roshan Deen G. Macromolecules 2000;33(21):7893–7.
[13] Peng T, Cheng YL. Polymer 2001;42(5):2091–100.
[14] Pinkrah VT, Snowden MJ, Mitchell JC, Seidel J, Chowdhry BZ, Fern GR. Langmuir 2003;19(3):585–90.
[15] Brazel CS, Peppas NA. Macromolecules 1995;28(24):8016–20.
[16] Brazel CS, Peppas NA. J Control Release 1996;39(1):57–64.
[17] Huglin MB, Liu Y, Velada JL. Polymer 1997;38(23):5785–91.
[18] Kono K, Okabe H, Morimoto K, Takagishi T. J Appl Polym Sci 2000;77(12):2703–10.

[19] Vakkalanka SK, Brazel CS, Peppas NA. J Biomater Sci Polym Ed 1996;8(2):119–29.
[20] Xue W, Champ S, Huglin MB. Polymer 2000;41(20):7575–81.
[21] Yang HH, Zhu QZ, Chen S, Li DH, Chen XL, Ding MT, et al. Anal Biochem 2001;296(2):167–73.
[22] Díez-Peña E, Quijada-Garrido I, Barrales-Rienda JM. Macromolecules 2002;35(23):8882–8.
[23] Díez-Peña E, Quijada-Garrido I, Barrales-Rienda JM. Polymer 2002;43(16):4341–8.
[24] Díez-Peña E, Quijada-Garrido I, Barrales-Rienda JM, Wilhelm M, Spiess HW. Macromol Chem Phys 2002;203(3):491–502.
[25] Díez-Peña E, Quijada-Garrido I, Frutos P, Barrales-Rienda JM. Macromolecules 2002;35(7):2667–75.
[26] Quijada-Garrido I, Prior-Cabanillas A, Garrido L, Barrales-Rienda JM. Macromolecules 2005;38(17):7434–42.
[27] Díez-Peña E, Quijada-Garrido I, Barrales-Rienda JM, Schnell I, Spiess HW. Macromol Chem Phys 2004;205(4):438–47.
[28] Díez-Peña E, Quijada-Garrido I, Barrales-Rienda JM. Macromolecules 2003;36(7):2475–83.
[29] Prior-Cabanillas A, Barrales-Rienda JM, Frutos G, Quijada-Garrido I. Polym Int 2007;56(4):506–11.
[30] Mansfield P, Bowtell R, Blackband S. J Magn Reson 1992;99(3):507–24.
[31] Melia CD, Rajabi-Siahboomi AR, Bowtell RW. Pharm Sci Technol Today 1998;1(1):32–9.
[32] Snaar JEM, Bowtell R, Melia CD, Morgan S, Narasimhan B, Peppas NA. Magn Reson Imaging 1998;16(5–6):691–4.
[33] Russo MAL, Strounina E, Waret M, Nicholson T, Truss R, Halley PJ. Biomacromolecules 2007;8(1):296–301.
[34] George KA, Wentrup-Byrne E, Hill DJT, Whittaker AK. Biomacromolecules 2004;5(4):1194–9.
[35] Knörgen M, Arndt KF, Richter S, Kuckling D, Schneider H. J Mol Struct 2000;554(1):69–79.
[36] Frisch HL. Polym Eng Sci 1980;20(1):2–13.
[37] Firestone BA, Siegel RA. J Appl Polym Sci 1991;43:901–4.
[38] Siegel RA. Adv Polym Sci 1993;109:233–67.
[39] Siegel RA. In: Kost J, editor. Pulsed and self-regulated drug delivery. Boca Raton, FL: CRC Press; 1990. p. 129–57.
[40] Falamarzian M, Firestone BA, Moxley BC. J Control Release 1988;8:179–82.
[41] Yoshida R, Okuyama Y, Sakai K, Okano T, Sakurai Y. J Membr Sci 1994;89:267–77.
[42] Okuyama Y, Yoshida R, Sakai K, Okano T, Sakurai Y. J Biomater Sci Polym Ed 1993;4:545–56.